Bilateral Boundary Control of Moving Shockwave in LWR Model of Congested Traffic

Huan Yu, Mamadou Diagne, *Member, IEEE,* Liguo Zhang, *Member, IEEE,*
Miroslav Krstic, *Fellow, IEEE*

***Abstract*—We develop backstepping state feedback control to stabilize a moving shockwave in a freeway segment under bilateral boundary actuations of traffic flow. A moving shockwave, consisting of light traffic upstream of the shockwave and heavy traffic downstream, is usually caused by changes of local road situations. The density discontinuity travels upstream and drivers caught in the shockwave experience transitions from free to congested traffic. Boundary control design in this paper brings the shockwave front to a static setpoint position, hindering the upstream propagation of traffic congestion. The traffic dynamics are described with Lighthill-Whitham-Richard (LWR) model, leading to a system of two first-order hyperbolic partial differential equations (PDEs). Each represents the traffic density of a spatial domain segregated by the moving interface. By Rankine-Hugoniot condition, the interface position is driven by flux discontinuity and thus governed by an ordinary differential equation (ODE) dependent on the PDE states. The control objective is to stabilize both the PDE states of traffic density and the ODE state of moving shock position to setpoint values. Using delay representation and backstepping method, we design predictor feedback controllers to cooperatively compensate state-dependent input delays to the ODE. From Lyapunov stability analysis, we show local stability of the closed-loop system in H^1 norm with an arbitrarily fast convergence rate. The stabilization result is demonstrated by a numerical simulation and the total travel time of the open-loop system is reduced by 12% in the closed-loop.**

***Index Terms*—Backstepping control, State-dependent delay compensation, PDE-ODE coupled system, Moving shockwave, LWR traffic model**

I. Introduction

Consider a common phenomenon in freeway traffic when there is a moving shockwave consisting of light traffic upstream of the shockwave and heavy traffic downstream. The shockwave conserves traffic flow at the interface of discontinuity and is caused by local changes of road situations like uphill and downhill gradients, curves, change of speed limits. The upstream propagation of the moving shockwave causes more and more vehicles entering into the congested traffic. Stabilizing the traffic congestion deals with many concerning aspects of the traffic such as fuel consumption, driving safety and comfort, CO_2 emissions. In this paper, we prevent the upstream propagation of traffic jams by designing boundary controllers that are implemented through traffic management infrastructures on freeways. Ramp metering and varying speed limit are most widely used to control traffic flux or velocity from the boundary of a stretch of freeway so that desirable traffic condition is achieved for inner domain of the freeway segment.

In developing boundary control strategies through ramp metering and varying speed limit, many recent efforts [5],[13],[21],[23],[24] are focused on macroscopic traffic models governed by PDE system. These model-based controllers regulate the evolution of traffic densities and velocities in order to dissipate traffic congestions on freeways. For instance, [21],[23] achieve the stabilization of stop-and-go traffic by second-order PDE model using boundary control.

Traffic discontinuity can be caused by various inhomogeneities of freeway or vehicles. Some studies consider it as a moving traffic flux constraint [9],[19] due to a reduction of road capacity. Slow moving vehicles, also known as moving bottlenecks, are represented in [6],[16],[22] with ODEs governing the velocity of slow vehicles. These are out of the scope of this paper and relevant to the controllability problem with boundary actuation. In this paper, we consider the situation where road capacity is conserved but shockwaves form due to changes of the road attributes. Dense traffic appears downstream of the shockwave front and the front of density discontinuity keeps moving upstream, driven by the flux discontinuity. The upstream propagation of the moving shockwave causes that traffic jams fully occupy the freeway segment. We aim to use boundary control inputs to "freeze" the upstream propagation of the traffic shockwave such that the total traffic congestion is reduced for the freeway segment.

In this work, we adopt the seminal Lighthill, Whitham and Richards (LWR) model which is a first-order, hyperbolic macroscopic PDE that describes the evolution of density. It is simple yet very powerful to describe the formation, dissipation and propagation of traffic shockwaves on the freeway. The shockwave consists of upstream, downstream traffic and a moving interface. The upstream and downstream traffic densities are governed by the LWR PDE models and the interface position is governed by Rankine-Hugoniot jump condition, leading to a density state-dependent nonlinear ODE. Therefore, we are dealing with a PDE-ODE coupled system, where the ODE state is dependent on the PDE states at the moving interface. The traffic flow is actuated at both boundaries of a freeway segment and are realized with on ramp metering. The control objective is to drive the moving interface to a desirable location and traffic states to steady values through bilateral boundary control inputs.

Huan Yu and Miroslav Krstic are with the Department of Mechanical and Aerospace Engineering, University of California, San Diego, 9500 Gilman Dr, La Jolla, CA 92093. Email: huy015@ucsd.edu, krstic@ucsd.edu

Mamadou Diagne is with the Department of Mechanical Aerospace and Nuclear Engineering, Rensselaer Polytechnic Institute, New York, 12180, USA. Email: diagnm@rpi.edu

Liguo Zhang is Faculty of Information Technology, Beijing University of Technology, Beijing, 100124, China. Email: zhangliguo@bjut.edu.cn. L. Zhang was supported by NSFC No.61873007, and BJNSF No.1182001.

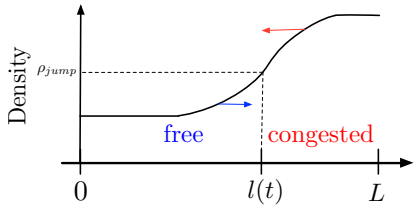

Fig. 1. Traffic moving shockwave front on freeway, the arrows represent propagation directions of density variations. In LWR model, the propagation directions are given by the characteristic speeds of density $Q'(\rho)$.

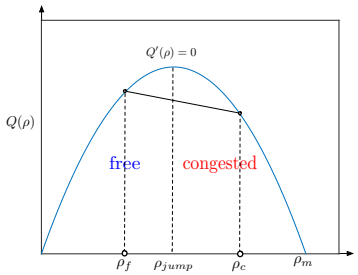

Fig. 2. Fundamental digram of traffic density and traffic flux relation.

Boundary control of PDE with state-dependent ODE systems has been intensively studied over the past few years. Backstepping control design method is used in solving these problems. In parabolic PDE system, the problem is known as Stefan problem with application to control of screw extruder for 3D Printing [15] and arctic sea ice temperature estimation [14]. In hyperbolic PDE system, theoretical results have been studied by [1],[3],[4],[11],[12],[18]. With application, [7] develops boundary control piston position in inviscid gas and [10] develops the control of a mass balance in screw extrusion process. Other applications include vibration suppression of mining cable elevator [20], control of Saint-Venant equation with hydraulic jumps [2]. Using Lyapunov analysis, [1] achieves the exponential stability in H^2 norm of a shock steady state for the inviscid Burgers equation by choosing appropriate feedback boundary conditions. However, the proposed method in [1] cannot be directly applied to the traffic shockwave problem due to the constraint on boundary feedback coefficients. Moreover, the application of the predictor feedback and backstepping control method in traffic shockwave problem has never been discussed before. In this paper, we propose state feedback bilateral controllers that achieves the local stability of the closed-loop system in H^1 norm with an arbitrarily fast convergence rate.

The contribution of this paper is twofold. This is the first theoretical result on applying backstepping methd to control two PDE state-dependent input delays to an ODE. Predictor-based state feedback design approach is adopted following [11],[18]. In fact, [18] shows a predictor feedback design for multiple constant delayed inputs to linear time-invariant systems while [11] considers a single implicitly defined state-dependent input delay to nonlinear time-invariant systems alternatively written as a PDE-ODE cascade system. In this work, we firstly present the predictor feedback design for two PDE states dependent input delays to an ODE. On the other hand, control problem of traffic moving shockwave has never been addressed before to author's best knowledge.

The outline of this paper: we introduce the LWR model to describe the moving shockwave problem. Then we obtain the state-dependent PDE-ODE model after linearization around steady states. The predictor state feedback control design follows and using Lyapunov analysis, we prove the local exponential stability of the closed-loop system. The result is validated with a numerical simulation.

II. Problem Statement

The moving shockwave front is the head of a shockwave, segregating traffic on a segment of freeway into two different schemes. The upstream traffic of the shockwave front is free and the downstream is congested, as shown in Fig.1. The traffic densities are described with the LWR model.

A. LWR traffic model

Traffic density $\rho(x,t)$ is governed by the following first-order nonlinear hyperbolic PDE, where $x \in [0, L]$, $t \in [0, \infty)$,

$$\partial_t \rho + Q'(\rho)\partial_x \rho = 0, \tag{1}$$

where $Q(\rho)$ is a fundamental diagram which shows the equilibrium relation of density and traffic flux. The fundamental diagram $Q(\rho)$ is defined as $Q(\rho) = \rho V(\rho)$. The equilibrium velocity $V(\rho)$ is an affine decreasing function of density which we choose the following Greenshield's model,

$$V(\rho) = v_m \left(1 - \frac{\rho}{\rho_m}\right), \tag{2}$$

where v_m is the maximum speed, ρ_m is the maximum density. The Greenshield's model $V(\rho)$ yields a strictly concave fundamental diagram $Q(\rho)$, shown in Fig. 2. The concavity of the fundamental diagram guarantees the hyperbolicity of the LWR model and the control designed proposed in this paper could be extended second-order traffic PDE models and other choices of strictly concave fundamental diagram. The jump density ρ_{jump} segregates densities into two sections, free regime on the left and congested regime on the right.

In the LWR PDE (1), density variations propagate with the characteristic speed $Q'(\rho)$. The free regime with light traffic, equivalently, $\rho_{\text{f}} < \rho_{\text{jump}}$, has its density variations transported downstream with $Q'(\rho)|_{\rho=\rho_{\text{f}}} = V(\rho_{\text{f}}) + \rho_{\text{f}} V'(\rho_{\text{f}}) > 0$, while the congested regime with denser traffic, namely, $\rho_{\text{c}} > \rho_{\text{jump}}$ has its density variations transported upstream with $Q'(\rho)|_{\rho=\rho_{\text{c}}} = V(\rho_{\text{c}}) + \rho_c V'(\rho_{\text{c}}) < 0$. As shown in Fig. 1, the moving shockwave considered here is the shock of a traffic wave, physically representing the discontinuity of density. The congested traffic density propagates upstream while the light traffic density propagates downstream. Therefore, the upstream front of the shockwave becomes steeper in propagation and eventually, the gradient $\partial_x \rho$ tends to be infinity [17]. In this context, drivers located in the upstream front of the shock will experience transition from the free to congested traffic. The position of the shockwave front is later defined by an ODE according to Rankine-Hugoniot condition.

B. Moving shockwave model

The moving shockwave model consists of upstream, downstream traffic densities and a moving interface located at the position of the density discontinuity. The dynamics of the upstream free traffic, the downstream congested traffic and the position of the moving interface are presented below.

Define the traffic density of the free regime as $\rho_{\rm f}(x,t)$ for $x \in [0, l(t)]$, $t \in [0, +\infty)$, and the congested regime as $\rho_{\rm c}(x,t)$, for $x \in [l(t), L]$, $t \in [0, +\infty)$, the LWR model that describes the traffic is given by

$$\partial_t \rho_{\rm f} + \partial_x(\rho_{\rm f} v_{\rm f}) = 0, \quad x \in [0, l(t)], \tag{3}$$

$$\partial_t \rho_{\rm c} + \partial_x(\rho_{\rm c} v_{\rm c}) = 0, \quad x \in [l(t), L], \tag{4}$$

where $l(t) \in [0, L]$ is the location of moving interface. The density and velocity relation is given by the Greenshield's model (2), $(i = {\rm f}, {\rm c})$,

$$v_i(x,t) = V_i(\rho_i(x,t)) = v_m \left(1 - \frac{\rho_i(x,t)}{\rho_m}\right). \tag{5}$$

Due to the flux discontinuity at the moving boundary, a traveling vehicle leaves the free regime to enter the congested regime. Dynamics of moving interface $l(t)$ is derived under the Rankine-Hugoniot condition which guarantees that the mass of traffic flow is conserved at the moving interface. The upstream propagation of the shockwave front is driven by the flux discontinuity,

$$\dot{l}(t) = \frac{\rho_{\rm c}(l(t),t) v_{\rm c}(l(t),t) - \rho_{\rm f}(l(t),t) v_{\rm f}(l(t),t)}{\rho_{\rm c}(l(t),t) - \rho_{\rm f}(l(t),t)}, \tag{6}$$

where the initial position of the shockwave front $0 < l(0) < L$. The following inequalities for initial conditions of PDEs (3),(4) are assumed: $\rho_{\rm c}(l(0),0) v_{\rm c}(l(0),0) < \rho_{\rm f}(l(0),0) v_{\rm f}(l(0),0)$, and $\rho_{\rm c}(l(0),0) > \rho_{\rm f}(l(0),0)$. Initially, the traffic downstream the interface is denser but with a smaller flux which lets less vehicles to pass through while the traffic upstream is light and let more vehicles to come in the segment. With the above assumptions to hold, we obtain from (6) that $\dot{l}(0) < 0$. The moving interface travels upstream, driven by a flux difference induced by the density discontinuity.

Substituting density-velocity relation (5) into (3),(4), and (6), we have two nonlinear PDEs and an ODE coupled system describing the dynamics of $\rho_{\rm f}(x,t)$, $\rho_{\rm c}(x,t)$ and $l(t)$ given by

$$\partial_t \rho_{\rm f}(x,t) = - v_m \partial_x \left(\rho_{\rm f}(x,t) - \frac{\rho_{\rm f}^2(x,t)}{\rho_m}\right), \tag{7}$$

$$\partial_t \rho_{\rm c}(x,t) = - v_m \partial_x \left(\rho_{\rm c}(x,t) - \frac{\rho_{\rm c}^2(x,t)}{\rho_m}\right), \tag{8}$$

$$\dot{l}(t) = v_m - \frac{v_m}{\rho_m}(\rho_{\rm c}(l(t),t) + \rho_{\rm f}(l(t),t)). \tag{9}$$

We consider the following controlled boundary condition for the nonlinear coupled PDE-ODE system consisting of (7), (8), and (9)

$$\rho_{\rm f}(0,t) = U_{\rm in}(t) + \rho_{\rm f}^\star, \tag{10}$$

$$\rho_{\rm c}(L,t) = U_{\rm out}(t) + \rho_{\rm c}^\star, \tag{11}$$

where we control the incoming and outgoing density variations of the freeway segment $U_{\rm in}(t)$ and $U_{\rm out}(t)$. The well-posedness of the system can be proved following [1] by defining a shock free solution to the quasilinear hyperbolic system (7)-(9) with compatibility condition verified by the initial conditions, which establish an equivalence relation with the shockwave solutions of the scalar Burgers equation. Our control objective is to stabilize both free and congested regime traffic $\rho_i(x,t)$ to uniform steady states $\rho_i^\star$ and at the same time, the moving interface $l(t)$ to a desirable static setpoint $l^\star$. Therefore, the shockwave becomes standstill within the freeway segment instead of moving upstream.

The incoming traffic flow needs to be in the free regime and the outgoing traffic flow is assumed to be congested downstream of the outlet. As mentioned in Section I, the control of density can be realized with on-ramp metering actuating the flux at both boundaries: we have at inlet $q_{\rm in}(t) = Q(\rho_{\rm f}(0,t))$, and at outlet $q_{\rm out}(t) = Q(\rho_{\rm c}(L,t))$. In practical implementation of the bilateral controllers, the flow variations of $q_{\rm ramp,in} = q_{\rm in}(t) - Q(\rho_{\rm f}^\star)$ and $q_{\rm ramp,out} = q_{\rm out}(t) - Q(\rho_{\rm c}^\star)$ are regulated with traffic lights on ramp.

Remark 1: For model validity, we assume that there exists a constant $L > 0$ such that the ODE state $l(t)$ satisfies

$$0 < l(t) < L, \tag{12}$$

so that (7),(8), and (9) are well-defined for $x \in [0, L]$, $t \in [0, +\infty)$. We emphasize that the proposed control law needs to guarantee the above condition.

III. State-dependent PDE-ODE Model

We linearize the original coupled PDE-ODE model $(\rho_{\rm f}(x,t), \rho_{\rm c}(x,t), l(t))$-system defined in (7),(8),(9) around steady states $(\rho_{\rm f}^\star, \rho_{\rm c}^\star, l^\star)$. The constant equilibrium setpoint values are chosen so that the following conditions that ensure the model validity hold

$$0 < \rho_{\rm f}^\star < \rho_{\rm jump} < \rho_{\rm c}^\star < \rho_m, \tag{13}$$

$$0 < l^\star < L. \tag{14}$$

At steady-state, the flux equilibrium needs to be achieved for both sides of the moving interface,

$$\rho_{\rm f}^\star V(\rho_{\rm f}^\star) = \rho_{\rm c}^\star V(\rho_{\rm c}^\star). \tag{15}$$

Using condition (15), the quadratic fundamental diagram yields that

$$\rho_{\rm f}^\star + \rho_{\rm c}^\star = \rho_m. \tag{16}$$

Define the state deviations from the system reference as

$$\tilde{\rho}_i(x,t) = \rho_i(x,t) - \rho_i^\star, \tag{17}$$

$$X(t) = l(t) - l^\star, \tag{18}$$

where $\dot{X}(t) = \dot{l}(t)$ is satisfied. Thus, the linearized PDE-ODE model (7)-(9) with the boundary conditions (10) and (11) around the system reference $(\rho_{\rm f}^\star, \rho_{\rm c}^\star, l^\star)$ is defined as the following $(\tilde{\rho}_{\rm f}(x,t), \tilde{\rho}_{\rm c}(x,t), X(t))$-system

$$\partial_t \tilde{\rho}_{\rm f}(x,t) = - u \partial_x \tilde{\rho}_{\rm f}(x,t), \quad x \in [0, l(t)], \tag{19}$$

$$\partial_t \tilde{\rho}_{\rm c}(x,t) = u \partial_x \tilde{\rho}_{\rm c}(x,t), \quad x \in [l(t), L], \tag{20}$$

$$\tilde{\rho}_{\rm f}(0,t) = U_{\rm in}(t), \tag{21}$$

$$\tilde{\rho}_{\rm c}(L,t) = U_{\rm out}(t), \tag{22}$$

$$\dot{X}(t) = - b\left(\tilde{\rho}_{\rm f}(l(t),t) + \tilde{\rho}_{\rm c}(l(t),t)\right), \tag{23}$$

where the transport speed is defined as

$$u = v_m \left(1 - \frac{2\rho_{\rm f}^\star}{\rho_m}\right), \tag{24}$$

and satisfy $0 < u < v_m$. The constant coefficient b in ODE is defined as $b = \frac{v_m}{\rho_m} > 0$. The model after linearization in (19)-(23) is a state-dependent coupled PDE-ODE system with

bilateral boundary control inputs from inlet and outlet. Notice that the PDE states are linearized around the steady states, but the ODE is dependent on PDE states and PDE states evolve in ODE-dependent space domain. Therefore the PDE-ODE coupled system (19)-(24) is a quasilinear system. The nonlinearity is geometrical and induced by the phase change between the free and congested regimes.

IV. Predictor-based control design

In this section, we first introduce the equivalent delay system representation to the system (19)-(23). Then, a backstepping transformation is applied to obtain predictor-based state feedback controls to compensate the PDE state-dependent delays to the ODE.

A. From coupled PDE-ODE to delay system representation

The system (19)-(23) can be represented by an unstable ODE with two distinct state-dependent input delays. Introduce the following state-dependent delays for the two transport PDEs

$$D_{\mathrm{f}}(t)=\frac{l(t)}{u},\quad D_{\mathrm{c}}(t)=\frac{L-l(t)}{u}, \tag{25}$$

where $l(t)=X(t)+l^{\star}$. The PDE states at $x=l(t)$ are represented by

$$\tilde{\rho}_{\mathrm{f}}(l(t),t)=&U_{\mathrm{in}}\left(t-D_{\mathrm{f}}(t)\right), \tag{26}$$
$$\tilde{\rho}_{\mathrm{c}}(l(t),t)=&U_{\mathrm{out}}\left(t-D_{\mathrm{c}}(t)\right), \tag{27}$$

where $U_{\mathrm{in}}(t)$ and $U_{\mathrm{out}}(t)$ are the boundary control inputs defined in (21) and (22) and the representations are valid when Remark 1 and Remark 3 hold and initial conditions are bounded as introduced in Theorem 1 later. The assumptions guarantee that the corresponding solution is defined for all $t\geq 0$, which implies that the moving interface $l(t)$ stays in the spatial domain before the control inputs reach it.

Substituting (26) and (27) into the ODE (23), the following state-dependent input delay system representation is derived

$$\dot{X}(t)=-b\left(U_{\mathrm{in}}(t-D_{\mathrm{f}}(X(t)))+U_{\mathrm{out}}(t-D_{\mathrm{c}}(X(t)))\right). \tag{28}$$

Remark 2: If the position of the moving shock front is close to the inlet half segment such that $l(t)\in\left[0,\frac{L}{2}\right]$, it holds that $\forall t\in[0,\infty), D_{\mathrm{f}}(t)\leq D_{\mathrm{c}}(t)$. As a result, delayed inlet control input $U_{\mathrm{in}}\left(t-D_{\mathrm{f}}(t)\right)$ reaches the moving shock front faster than delayed outlet control input $U_{\mathrm{out}}\left(t-D_{\mathrm{c}}(t)\right)$. If $l(t)\in\left[\frac{L}{2},L\right]$, $\forall t\in[0,\infty), D_{\mathrm{f}}(t)\geq D_{\mathrm{c}}(t)$ holds. Then $U_{\mathrm{out}}\left(t-D_{\mathrm{c}}(t)\right)$ reaches the moving shock front faster than $U_{\mathrm{in}}\left(t-D_{\mathrm{f}}(t)\right)$.

We introduce a new coordinate z defined as

$$z=\begin{cases}\dfrac{l(t)-x}{u}, & x\in[0,l(t)],\\ \dfrac{x-l(t)}{u}, & x\in[l(t),L],\end{cases} \tag{29}$$

and new variables $\tilde{\varrho}_{\mathrm{f}}(z,t)$ and $\tilde{\varrho}_{\mathrm{c}}(z,t)$ defined in z-coordinate. The transformations between $\tilde{\rho}_{\mathrm{f}}(x,t),\tilde{\rho}_{\mathrm{c}}(x,t)$ and $\tilde{\varrho}(z,t),\tilde{\varrho}_{c}(z,t)$ are given by

$$\tilde{\varrho}_{\mathrm{f}}(z,t)=&\tilde{\rho}_{\mathrm{f}}(l(t)-uz,t),\quad z\in[0,D_{\mathrm{f}}(t)], \tag{30}$$
$$\tilde{\varrho}_{\mathrm{c}}(z,t)=&\tilde{\rho}_{\mathrm{c}}(l(t)+uz,t),\quad z\in[0,D_{\mathrm{c}}(t)], \tag{31}$$

and the associated inverse transformations of (30) and (31) are given by

$$\tilde{\rho}_{\mathrm{f}}(x,t)=&\tilde{\varrho}_{\mathrm{f}}\left(\frac{l(t)-x}{u},t\right),\quad x\in[0,l(t)], \tag{32}$$
$$\tilde{\rho}_{\mathrm{c}}(x,t)=&\tilde{\varrho}_{\mathrm{c}}\left(\frac{x-l(t)}{u},t\right),\quad x\in[l(t),L]. \tag{33}$$

Using (30) and (31), the original system (19)-(23) is rewritten in the new z-coordinate as

$$\partial_t\tilde{\varrho}_{\mathrm{f}}(z,t)=\left(1-\frac{\dot{l}(t)}{u}\right)\partial_z\tilde{\varrho}_{\mathrm{f}}(z,t),\ z\in[0,D_{\mathrm{f}}(t)], \tag{34}$$
$$\partial_t\tilde{\varrho}_{\mathrm{c}}(z,t)=\left(1+\frac{\dot{l}(t)}{u}\right)\partial_z\tilde{\varrho}_{\mathrm{c}}(z,t),\ z\in[0,D_{\mathrm{c}}(t)], \tag{35}$$
$$\tilde{\varrho}_{\mathrm{f}}(D_{\mathrm{f}}(t),t)=&U_{\mathrm{in}}(t), \tag{36}$$
$$\tilde{\varrho}_{\mathrm{c}}(D_{\mathrm{c}}(t),t)=&U_{\mathrm{out}}(t), \tag{37}$$

with the ODE state $l(t)=X(t)+l^{\star}$ given by

$$\dot{X}(t)=-b\left(\tilde{\varrho}_{\mathrm{f}}(0,t)+\tilde{\varrho}_{\mathrm{c}}(0,t)\right). \tag{38}$$

Remark 3: The proposed control laws U_{in} and U_{out} need to designed such that the following condition for the ODE state $l(t)$ is guaranteed

$$-u<\dot{l}(t)<u, \tag{39}$$

so that well-posedness of the system (34)-(38) for $x\in[0,L]$, $t\in[0,+\infty)$ is guaranteed.

Based on the above system in delay representation, we construct the following predictor-based backstepping transformation so that the delays are compensated with the control design.

B. Predictor-based backstepping transformation

We consider the following backstepping transformation, motivated by the predictor-based transformation for delay representation $\varrho_{\mathrm{f}}(z,t)$ and $\varrho_{\mathrm{c}}(z,t)$ defined in (34)-(37),

$$\omega_{\mathrm{f}}(z,t)=&\tilde{\varrho}_{\mathrm{f}}(z,t)-K_{\mathrm{f}}\Bigg(X(t)-b\int_0^z\tilde{\varrho}_{\mathrm{f}}(\xi,t)d\xi\\&-b\int_0^{\min\{D_{\mathrm{c}}(t),z\}}\tilde{\varrho}_{\mathrm{c}}(\xi,t)d\xi\Bigg),\quad z\in[0,D_{\mathrm{f}}(t)], \tag{40}$$
$$\omega_{\mathrm{c}}(z,t)=&\tilde{\varrho}_{\mathrm{c}}(z,t)-K_{\mathrm{c}}\Bigg(X(t)-b\int_0^z\tilde{\varrho}_{\mathrm{c}}(\xi,t)d\xi\\&-b\int_0^{\min\{D_{\mathrm{f}}(t),z\}}\tilde{\varrho}_{\mathrm{f}}(\xi,t)d\xi\Bigg),\quad z\in[0,D_{\mathrm{c}}(t)], \tag{41}$$

where $K_{\mathrm{f}},K_{\mathrm{c}}>0$ are positive constant gain kernels. The above transformation in the original PDE state variables

$\rho_{\rm f}(x,t)$ for $x\in[0,l(t)]$ and $\rho_{\rm c}(x,t)$ for $x\in[l(t),L]$, is given by

$$w_{\rm f}(x,t)=\tilde{\rho}_{\rm f}(x,t)-K_{\rm f}\bigg(X(t)-\frac{b}{u}\int_x^{l(t)}\tilde{\rho}_{\rm f}(\xi,t)d\xi -\frac{b}{u}\int_{l(t)}^{\min\{L,2l(t)-x\}}\tilde{\rho}_{\rm c}(\xi,t)d\xi\bigg),\quad x\in[0,l(t)], \tag{42}$$

$$w_{\rm c}(x,t)=\tilde{\rho}_{\rm c}(x,t)-K_{\rm c}\bigg(X(t)-\frac{b}{u}\int_{l(t)}^{x}\tilde{\rho}_{\rm c}(\xi,t)d\xi -\frac{b}{u}\int_{\max\{0,2l(t)-x\}}^{l(t)}\tilde{\rho}_{\rm f}(\xi,t)d\xi\bigg),\quad x\in[l(t),L]. \tag{43}$$

- For the case $D_{\rm f}(t)\le D_{\rm c}(t)$, it follows that $l(t)\in\big[0,\frac{L}{2}\big]$ and the following holds

$$x\in[0,l(t)]\implies\min\{L,2l(t)-x\}=2l(t)-x. \tag{44}$$

- For the case $D_{\rm f}(t)\ge D_{\rm c}(t)$, it follows that $l(t)\in\big[\frac{L}{2},L\big]$, the following holds

$$x\in[l(t),L]\implies\max\{0,2l(t)-x\}=2l(t)-x. \tag{45}$$

Later on, two pairs of state feedback controllers are obtained respectively for $l(t)\in\big[0,\frac{L}{2}\big]$ and $l(t)\in\big[\frac{L}{2},L\big]$. The inverse transformation of (42),(43) is given by

$$\tilde{\rho}_{\rm f}(x,t)=w_{\rm f}(x,t)+K_{\rm f}\bigg(X(t)-\frac{b}{u}\int_x^{l(t)}w_{\rm f}(\xi,t)d\xi -\frac{b}{u}\int_{l(t)}^{\min\{L,2l(t)-x\}}w_{\rm c}(\xi,t)d\xi\bigg),\ x\in[0,l(t)], \tag{46}$$

$$\tilde{\rho}_{\rm c}(x,t)=w_{\rm c}(x,t)+K_{\rm c}\bigg(X(t)-\frac{b}{u}\int_{l(t)}^{x}w_{\rm c}(\xi,t)d\xi -\frac{b}{u}\int_{\max\{0,2l(t)-x\}}^{l(t)}w_{\rm f}(\xi,t)d\xi\bigg),\quad x\in[l(t),L]. \tag{47}$$

The derivation of the inverse transformation is straightforward following [11], [18] and thus omitted here. Let us denote the above transformations as

$$\tilde{\rho}_{\rm f}=\mathcal{T}_{\rm f}[w_{\rm f},w_{\rm c}], \tag{48}$$
$$\tilde{\rho}_{\rm c}=\mathcal{T}_{\rm c}[w_{\rm f},w_{\rm c}]. \tag{49}$$

At the moving interface, we have

$$w_{\rm f}(l(t),t)=\tilde{\rho}_{\rm f}(l(t),t)-K_{\rm f}X(t), \tag{50}$$
$$w_{\rm c}(l(t),t)=\tilde{\rho}_{\rm c}(l(t),t)-K_{\rm c}X(t). \tag{51}$$

We take temporal and spatial derivative on both sides of (42),(43) and substitute into the PDE-ODE original system (19)-(23). With the designed bilateral boundary controllers $U_{\rm in}$ and $U_{\rm out}$ introduced later, we obtain the target system satisfied by $w_{\rm f}(x,t)$ and $w_{\rm c}(x,t)$,

$$\partial_t w_{\rm f}+u\partial_x w_{\rm f}=\frac{K_{\rm f}b}{u}\dot{l}(t)(g(t)+2\epsilon_c(x,t)),\ x\in[0,l(t)], \tag{52}$$

$$\partial_t w_{\rm c}-u\partial_x w_{\rm c}=\frac{K_{\rm c}b}{u}\dot{l}(t)(g(t)-2\epsilon_{\rm f}(x,t)),\ x\in[l(t),L], \tag{53}$$

$$w_{\rm f}(0,t)=0, \tag{54}$$
$$w_{\rm c}(L,t)=0, \tag{55}$$
$$\dot{X}(t)=-aX(t)-b\left(w_{\rm c}(l(t),t)+w_{\rm f}(l(t),t)\right), \tag{56}$$

where (54),(55) are the controlled boundaries and the constant coefficient $a=b(K_{\rm f}+K_{\rm c})>0$ is obtained by substituting (50),(51) into (23), given $b,K_{\rm f},K_{\rm c}>0$. The time-varying term $g(t)$ is defined as

$$g(t)=(K_{\rm f}-K_{\rm c})X(t)+w_{\rm f}(l(t),t)-w_{\rm c}(l(t),t), \tag{57}$$

and the space and time-varying terms $\epsilon_{\rm c}(x,t)$ and $\epsilon_{\rm f}(x,t)$ are given by

$$\epsilon_{\rm c}(x,t)=\tilde{\rho}_{\rm c}(2l(t)-x,t)=\mathcal{T}_{\rm c}[w_{\rm f},w_{\rm c}](2l(t)-x,t), \tag{58}$$
$$\epsilon_{\rm f}(x,t)=\tilde{\rho}_{\rm f}(2l(t)-x,t)=\mathcal{T}_{\rm f}[w_{\rm f},w_{\rm c}](2l(t)-x,t). \tag{59}$$

We assume that densities outside freeway segment $[0,L]$ are at steady states, therefore $\tilde{\rho}_{\rm c}(2l(t)-x,t)=0$ when $2l(t)-x>L$, and $\tilde{\rho}_{\rm f}(2l(t)-x,t)=0$ when $2l(t)-x<0$. Hence, the followings hold for $\epsilon_{\rm f}(x,t)$ and $\epsilon_{\rm c}(x,t)$,

$$\begin{cases}\epsilon_{\rm f}(x,t)=0, & l(t)\in(0,L/2)\ \text{ and }\ x\in[2l(t),L],\\ \epsilon_{\rm c}(x,t)=0, & l(t)\in(L/2,L)\ \text{and}\ \ x\in[0,2l(t)-L].\end{cases} \tag{60}$$

Otherwise, $\epsilon_{\rm f}(x,t)$ and $\epsilon_{\rm c}(x,t)$ are given by expressions in (58) and (59). The bilateral state feedback boundary actuations for inlet and outlet of the segment are derived from (42),(43) and (54),(55) as

$$U_{\rm in}(t)=K_{\rm f}\bigg(X(t)-\frac{b}{u}\int_0^{l(t)}\tilde{\rho}_{\rm f}(\xi,t)d\xi-\frac{b}{u}\int_{l(t)}^{\min\{L,2l(t)\}}\tilde{\rho}_{\rm c}(\xi,t)d\xi\bigg), \tag{61}$$

$$U_{\rm out}(t)=K_{\rm c}\bigg(X(t)-\frac{b}{u}\int_{l(t)}^{L}\tilde{\rho}_{\rm c}(\xi,t)d\xi-\frac{b}{u}\int_{\max\{0,2l(t)-L\}}^{l(t)}\tilde{\rho}_{\rm f}(\xi,t)d\xi\bigg). \tag{62}$$

We obtain two pairs of controller designs for $l(t)\in\big[0,\frac{L}{2}\big]$ and $l(t)\in\big[\frac{L}{2},L\big]$, respectively. When $l(t)\in\big[0,\frac{L}{2}\big]$, it holds true that $\min\{L,2l(t)\}=2l(t),\max\{0,2l(t)-L\}=0$ and when $l(t)\in\big[\frac{L}{2},L\big]$ one gets $\min\{L,2l(t)\}=L,\max\{0,2l(t)-x\}=2l(t)$.

In addition, when $l(t)=\frac{L}{2}$, controller integral forms become identical for $l(t)\in\big[0,\frac{L}{2}\big]$ and $l(t)\in\big[\frac{L}{2},L\big]$: $U_{\rm in}(t)=K_{\rm f}\Big(X(t)-\frac{b}{u}\int_0^{\frac{L}{2}}\tilde{\rho}_{\rm f}(\xi,t)d\xi-\frac{b}{u}\int_{\frac{L}{2}}^{L}\tilde{\rho}_{\rm c}(\xi,t)d\xi\Big)$, and $U_{\rm out}(t)=K_{\rm c}\Big(X(t)-\frac{b}{u}\int_0^{\frac{L}{2}}\tilde{\rho}_{\rm f}(\xi,t)d\xi-\frac{b}{u}\int_{\frac{L}{2}}^{L}\tilde{\rho}_{\rm c}(\xi,t)d\xi\Big)$. Note that the bilateral control input continuously switches between the above control laws when the moving interface position passes through the middle of the freeway segment.

Due to the invertibility of the transformation in (42),(43), stability of the target system $(w_{\rm c}(x,t), w_{\rm f}(x,t), X(t))$ and stability the plant $(\tilde{\rho}_{\rm f}(x,t), \tilde{\rho}_{\rm c}(x,t), X(t))$ are equivalent. In the next section, we apply Lyapunov analysis to prove the stability of the target system. Define the H^1-norm $||f(\cdot,t)||_{H^1_{(a,b)}}$ as $||f(\cdot,t)||_{H^1_{(a,b)}} = \sqrt{\left(\int_a^b f^2(x,t) + f_x^2(x,t)dx\right)}$. We now state the main result of the paper.

Theorem 1: Consider a closed-loop system consisting of the PDE-ODE system (19)-(23) and the bilateral full-state feedback control laws for inlet and outlet (61),(62). For any system reference $(\rho_{\rm f}^\star, \rho_{\rm c}^\star, l^\star) \in H^1((0,l^\star);\mathbb{R}) \times H^1((l^\star,L);\mathbb{R})) \times (0,L)$ which satisfies conditions (13), (14) and (16), and for any given $L>0$, there exist $c>0,\ \gamma>0,\ \zeta>0$ such that if the initial conditions of the system $(\rho_{\rm f}(x,0), \rho_{\rm c}(x,0), l(0))$ satisfy $Z(0)<\zeta$, local exponential stability with an arbitrary fast convergence rate of the closed-loop system with bilateral control laws holds $\forall t \in [0,\infty)$, namely,

$$Z(t) \le ce^{-\gamma t} Z(0), \tag{63}$$

where $Z(t)$ is defined as $Z(t) = ||\rho_{\rm f}(x,t) - \rho_{\rm f}^\star||_{H^1_{[0,l(t)]}} + ||\rho_{\rm c}(x,t) - \rho_{\rm c}^\star||_{H^1_{[l(t),L]}} + |l(t)-l^\star|^2$, and conditions (12),(39) are satisfied for model validity.

V. Proof of Theorem 1

In the proof, local stability of the closed-loop system in the H^1 sense is shown with Lyapunov analysis and the conditions (12),(39) are guaranteed by our control design. The proof of Theorem 1 is established through following steps: we firstly prove the local stability of the target system (52)-(56) given time interval $\forall t \in [0, t^\star)$ under the assumption that conditions (12),(39) are satisfied. Then we prove that with the initial conditions of states variables bounded, the local exponential stability of the above target system holds for $\forall t \in [0,+\infty)$ with the assumption removed. This is achieved by comparison principle and contradiction proof in Lemma 3. In the end, the stability analysis of the target system yields the stability of original PDE-ODE system in (7)-(9).

Let us define the Lyapunov functional

$$V(t) = V_1(t) + V_2(t) + V_3(t) + V_4(t) + c_5 V_5(t), \tag{64}$$

where $\lambda > 0$ with the component Lyapunov functions

$$V_1(t) = \int_0^{l(t)} e^{-c_1 x} w_{\rm f}^2(x,t)dx, \tag{65}$$

$$V_2(t) = \int_{l(t)}^{L} e^{c_2(x-L)} w_{\rm c}^2(x,t)dx, \tag{66}$$

$$V_3(t) = \int_0^{l(t)} e^{-c_3 x} \partial_x w_{\rm f}^2(x,t)dx, \tag{67}$$

$$V_4(t) = \int_{l(t)}^{L} e^{c_4(x-L)} \partial_x w_{\rm c}^2(x,t)dx, \tag{68}$$

$$V_5(t) = X(t)^2. \tag{69}$$

Lemma 1: Assume $\exists t^\star > 0$ such that for all $t \in [0,t^\star]$ the conditions (12),(39) are satisfied, then there exists $\sigma > 0$ such that the following holds $\forall t \in [0,t^\star)$,

$$\dot{V}(t) \le -\sigma V + \tau V^{3/2} + \theta V^2. \tag{70}$$

Proof: Taking time derivative of the Lyapunov function (64) along the solution of the target system (52)-(56) and using the inequality (39), we have

$$\begin{aligned}\dot{V}_1(t) =& -c_1 u \int_0^{l(t)} e^{-c_1 x} w_{\rm f}^2(x,t)dx \\ &+ \frac{2K_{\rm f} b}{u} \dot{l}(t) g(t) \int_0^{l(t)} e^{-c_1 x} w_{\rm f}(x,t)dx \\ &+ \frac{4K_{\rm f} b}{u} \dot{l}(t) \int_0^{l(t)} e^{-c_1 x} \epsilon_{\rm c}(x,t) w_{\rm f}(x,t)dx, \end{aligned} \tag{71}$$

$$\begin{aligned}\dot{V}_2(t) =& -c_2 u \int_{l(t)}^{L} e^{c_2(x-L)} w_{\rm c}^2(x,t)dx \\ &+ \frac{2K_{\rm c} b}{u} \dot{l}(t) g(t) \int_{l(t)}^{L} e^{c_2(x-L)} w_{\rm c}(x,t)dx \\ &- \frac{4K_{\rm c} b}{u} \dot{l}(t) \int_{l(t)}^{L} e^{c_2(x-L)} \epsilon_{\rm f}(x,t) w_{\rm c}(x,t)dx, \end{aligned} \tag{72}$$

$$\begin{aligned}\dot{V}_3(t) =& -c_3 u \int_0^{l(t)} e^{-c_3 x} \partial_x w_f^2(x,t)dx + u\partial_x w_{\rm f}^2(0,t) \\ &+ \frac{4K_{\rm f} b}{u} \dot{l}(t) \int_0^{l(t)} e^{-c_3 x} \partial_x \epsilon_{\rm c}(x,t) \partial_x w_{\rm f}(x,t)dx, \end{aligned} \tag{73}$$

$$\begin{aligned}\dot{V}_4(t) =& -c_4 u \int_{l(t)}^{L} e^{c_4(x-L)} \partial_x w_{\rm c}^2(x,t)dx + u\partial_x w_{\rm c}^2(L,t) \\ &- \frac{4K_{\rm c} b}{u} \dot{l}(t) \int_{l(t)}^{L} e^{c_4(x-L)} \partial_x \epsilon_{\rm c}(x,t) \partial_x w_{\rm c}(x,t)dx, \end{aligned} \tag{74}$$

$$\dot{V}_5(t) = -2aX(t)^2 - 2b\left(w_{\rm c}(l(t),t) + w_{\rm f}(l(t),t)\right) X(t). \tag{75}$$

Using the boundary conditions (54)(55), Agmon's inequality, Young's inequality and Poincaré inequality, we obtain the following

$$w_{\rm f}^2(l(t),t) \le ||w_{\rm f}||_\infty^2 \le 4||\partial_x w_{\rm f}||_2^2 \le 4e^{c_3 L} V_3, \tag{76}$$

$$w_{\rm c}^2(l(t),t) \le ||w_{\rm c}||_\infty^2 \le 4||\partial_x w_{\rm c}||_2^2 \le 4e^{c_4 L} V_4. \tag{77}$$

Plugging the above inequalities into the ODE (56) yields that there exists $\delta > 0$ such that

$$|\dot{l}(t)| \le a\sqrt{V_5} + 2b(\sqrt{e^{c_3 L} V_3} + \sqrt{e^{c_4 L} V_4}) \le \delta\sqrt{V}. \tag{78}$$

Using Young's inequality, Cauchy-Schwarz inequality for (57) and (76),(77), there exists $\mu > 0$,

$$g(t)^2 \le 2((K_f - K_c)^2 V_5 + 4e^{c_3 L} V_3 + 4e^{c_4 L} V_4) \le \mu V, \tag{79}$$

By definition of $\epsilon_{\rm c}(x,t)$ in (58), there exist $\eta > 0$, such that

$$\int_0^{l(t)} \epsilon_{\rm c}^2(x,t)dx \le \eta V. \tag{80}$$

It follows that

$$\begin{aligned}\dot{V}_1(t) \le& -c_1 u V_1 + \frac{2K_{\rm f} b}{u} |\dot{l}(t)| \left(g^2(t) + \int_0^{l(t)} w_{\rm f}^2(x,t)dx\right) \\ &+ \frac{4K_{\rm f} b}{u} |\dot{l}(t)| \left(\int_0^{l(t)} \epsilon_{\rm c}^2(x,t)dx + \int_0^{l(t)} w_{\rm f}^2(x,t)dx\right), \end{aligned} \tag{81}$$

Plugging (79) and (80) into the above inequality, there exists $\kappa_1 > 0$ such that

$$\dot{V}_1(t) \leq -c_1 u V_1 + \kappa_1 V^{3/2}, \tag{82}$$

Taking total time derivative of boundary condition (54) yields,

$$\partial_x w_{\rm f}(0,t) = \frac{K_{\rm f} b}{u^2} \dot{l}(t)(g(t) + 2\epsilon_{\rm c}(0,t)), \tag{83}$$

where it holds that $\epsilon_{\rm c}(0,t) = 0$, according to the definition (60). Given the definition of $\epsilon_{\rm c}(x,t)$ in (58), there exist $\nu > 0$ such that

$$\int_0^{l(t)} \partial_x \epsilon_{\rm c}^2(x,t) dx \leq \nu V. \tag{84}$$

Using Young's inequality and plugging (78), (79) into (83), we obtain that there exists $\theta_1 > 0$ such that

$$\partial_x w_{\rm f}^2(0,t) \leq \frac{K_{\rm c}^2 b^2}{u^4} |\dot{l}(t)|^2 g^2(t) \leq \theta_1 V^2, \tag{85}$$

Plugging (76), (78), (84) and (85) into (73), we obtain that there exists $\kappa_3 > 0$ such that

$$\dot{V}_3(t) \leq -uV_3 + \kappa_3 V^{3/2} + \theta_1 V^2, \tag{86}$$

In the same fashion, we could obtain that there exist $\kappa_2, \kappa_4 > 0$ and $\theta_2 > 0$ such that

$$\dot{V}_2(t) \leq -uV_2 + \kappa_2 V^{3/2}, \tag{87}$$

$$\dot{V}_4(t) \leq -uV_4 + \kappa_4 V^{3/2} + \theta_2 V^2, \tag{88}$$

For the last Lyapunov component, the following holds

$$\dot{V}_5(t) \leq -\left(2a - \frac{a}{2} - \frac{a}{2}\right) V_5 + \frac{8e^{c_3 L} b^2}{a} V_3 + \frac{8e^{c_4 L} b^2}{a} V_4. \tag{89}$$

Substituting inequalities (82) and (86)-(89) into (64), it follows that

$$\begin{aligned} \dot{V}(t) \leq & -c_1 u V_1 - c_2 u V_2 - \left(c_3 u - c_5 \frac{8e^{c_3 L} b^2}{a}\right) V_3 \\ & - \left(c_4 u - c_5 \frac{8e^{c_4 L} b^2}{a}\right) V_4 - c_5 a V_5 + \tau V^{3/2} + \theta V^2. \end{aligned} \tag{90}$$

where $\tau = \kappa_1 + \kappa_2 + \kappa_3 + \kappa_4 > 0$ and $\theta = \theta_1 + \theta_2$. We choose c_5 such that $c_5 = \min\left\{\frac{c_3 a u}{16b^2} e^{-c_3 L}, \frac{c_4 a u}{16b^2} e^{-c_4 L}\right\}$, thus it holds for $\sigma = \min\left\{c_1 u, c_2 u, \frac{c_3 u}{2}, \frac{c_4 u}{2}, a\right\}$,

$$\dot{V}(t) \leq -\sigma V + \tau V^{3/2} + \theta V^2. \tag{91}$$

□

Lemma 2: The inequality (70) yields that for any $V(0) < \delta_0$ where $\delta_0 = \frac{-\tau + \sqrt{\tau^2 + 2\sigma\theta}}{2\theta}$, then it holds that

$$\dot{V}(t) \leq -\frac{\sigma}{2} V. \tag{92}$$

By comparison principle, the exponential stability is satisfied that $\forall t \in [0, t^\star)$,

$$V(t) \leq V(0) e^{-\frac{\sigma}{2} t} < \delta_0. \tag{93}$$

Recall $a = b(K_{\rm f} + K_{\rm c})$. the control gains $K_{\rm f}$ and $K_{\rm c}$ and the coefficients $c_i, i = 1,2,3,4$ can be chosen arbitrarily large such that an arbitrarily fast convergence rate $\frac{\sigma}{2}$ could be achieved, namely, rapid stabilization for the closed-loop system.

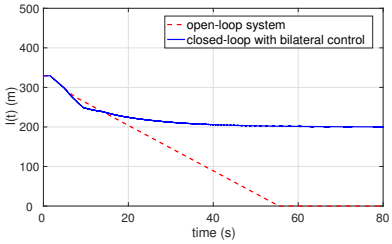

Fig. 3. Evolution of the moving interface position $l(t)$ for open-loop system and for closed-loop system with bilateral boundary control.

Lemma 3: If the initial conditions of the target system $(w_{\rm f}(x,0), w_{\rm c}(x,0), X(0))$ satisfy the following

$$V(0) < \min\{\delta_0, \delta_1, \delta_2\}, \tag{94}$$

where the positive constant δ_1 is defined as

$$\delta_1 = \min\left\{(L - l^\star)^2, (l^\star)^2\right\}, \quad \delta_2 = \frac{u^2}{\delta^2}. \tag{95}$$

Then Lyapunov functional inequality (92) and conditions (12),(39) hold for $t \in [0, \infty)$.

Proof: We assume that there exists $t^\star > 0$ such that condition (12) is satisfied for $t \in [0, t^\star)$ but is violated at $t = t^\star$. Given (94) and by comparison principle, the following inequality holds

$$V(t^\star) \leq V(0) < \delta_1. \tag{96}$$

According to the definition of $V(t)$ in (64), we obtain that $X^2(t^\star) \leq V(t^\star)$. Combining (95) and (96), we have

$$X^2(t^\star) < \delta_1 = \min\left\{(L - l^\star)^2, (l^\star)^2\right\}. \tag{97}$$

Since $l(t^\star) = X(t^\star) + l^\star$ and $0 < l^\star < L$, we obtain from (97) that

$$0 < l(t^\star) < L. \tag{98}$$

We conclude that (98) contradicts the assumption that (12) is violated at $t = t^\star$. Therefore, the condition (12) is guaranteed for $t \in [0, \infty)$ when the initial condition $V(0)$ satisfies (94). By inequality (78), we have $|\dot{l}(t^\star)|^2 \leq \delta^2 V(t^\star)$. Given (94), it holds that $V(t^\star) \leq V(0) < \frac{u^2}{\delta^2}$. Thus we have $|\dot{l}(t^\star)|^2 < u^2$ and it follows that

$$-u < \dot{l}(t) < u. \tag{99}$$

This completes the proof Lemma 3. Due to invertibility of the transformation in (42),(43), we conclude that the system (19)-(23) with control laws (61),(62) is locally exponentially stable in the H^1 norm, which completes the proof of Theorem 1. □

VI. Simulation

We simulate the proposed control design considering a moving traffic shockwave in a 500-meter freeway segment. The maximum velocity is $v_m = 144$ km/hr and maximum density is $\rho_m = 160$ vehs/km. The initial traffic profile and the desirable target traffic profile $\rho_{\rm f}^\star = 32$ vehs/km, $\rho_{\rm c}^\star = 128$ vehs/km, $l^\star = 0.2$ km, $\rho_{\rm jump} = 80$ vehs/km are shown in Fig. 4, where the position of the shockwave front is initially

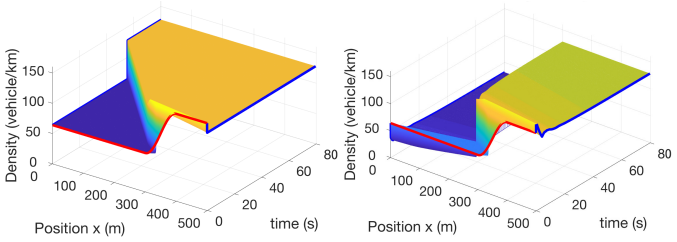

Fig. 4. Evolution of traffic density PDE states for the open-loop system on left and for the closed-loop system on right. Traffic density profile for initial condition with a soft shockwave is highlighted with color red and the target profile is that there is a shock steady state located at $x = 200$ m where its upstream is free and its downstream congested, shown on the right after 50s.

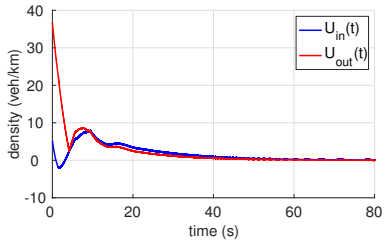

Fig. 5. Evolution of bilateral control inputs over time.

located at 330-meter and the final setpoint location is at 200-meter, as shown in Fig. 3. The initial position of the shockwave front is in the right-half plane of the segment while its final position is located at the left-half plane. The control objective is to regulate PDE states and ODE state from the initial profile to the reference profile, as shown in Fig. 4. After around $50s$, the moving interface position stops at the setpoint location $l = 200$ m with bilateral control while in open-loop system it propagates upstream and travels out of the freeway segment before 1 min in Fig. 3. In Fig. 4, PDE density states of the whole segment becomes congested in the open-loop system while the upstream traffic remains to be free in the closed-loop system. In Fig. 5, one can observe that the bilateral control signals also converge to zeros after around $50s$. In addition, total travel time (TTT) as $\mathrm{TTT} = \int_0^{80s}\int_0^L \rho(x,t)dxdt$ is defined in [17] and the closed-loop system reduces the total travel time by 12%, compared with the open-loop.

VII. Conclusion

This paper addresses boundary feedback control problem of moving shockwave in congested traffic described by an PDE-ODE system. To stabilize the coupled system to a desired setpoint, we use predictor-based backstepping method to transform the state-dependent PDE-ODE coupled system to a target system, where the PDE state-dependent input delays to ODE are compensated by the bilateral boundary control inputs to PDEs. Actuations of traffic densities at both boundaries are considered. The local exponential stability in H^1 norm with an arbitrarily fast converegence rate is achieved. For future work, general theoretical results on multiple PDEs state-dependent input delays cascading to a nonlinear ODE and consideration of different characteristic speeds of the free flow and congested flow are of authors' interest.

Acknowledgments

Huan Yu would like to thank Dr. Stephen Chen and Dr. Shumon Koga for the fruitful discussions of this work.

References

[1] G. Bastin, J. M. Coron, A. Hayat, & P. Shang. "Exponential boundary feedback stabilization of a shock steady state for the inviscid Burgers equation". *Mathematical Models and Methods in Applied Sciences*, vol. 29, no.2, pp.271-316, 2019.

[2] G. Bastin, J. M. Coron, A. Hayat, & P. Shang. "Boundary feedback stabilization of hydraulic jumps". *IFAC Journal of Systems and Control*, 100026, 2019.

[3] N. Bekiaris-Liberis, & M. Krstic. "Compensation of state-dependent input delay for nonlinear systems". *IEEE Transactions on Automatic Control*, vol.58(2), pp.275-289, 2013.

[4] N. Bekiaris-Liberis, & M. Krstic. "Predictor-feedback stabilization of multi-input nonlinear systems". *IEEE Transactions on Automatic Control*,vol.62(2), pp.516–531, 2017.

[5] F. Belletti, M. Huo, X. Litrico, & A. M. Bayen. "Prediction of traffic convective instability with spectral analysis of the Aw–Rascle–Zhang model," *Physics Letters A*, vol.379(38), pp.2319-2330, 2015.

[6] R. Borsche, R. M. Colombo, & M. Garavello. "Mixed systems: ODEs–balance laws". *Journal of Differential equations*, vol.252(3), pp.2311-2338, 2012.

[7] M. Buisson-Fenet, S. Koga, & M. Krstic. "Control of Piston Position in Inviscid Gas by Bilateral Boundary Actuation," *In 2018 IEEE Conference on Decision and Control (CDC)*, pp. 5622-5627, 2018.

[8] X. Cai, & M. Krstic. "Nonlinear control under wave actuator dynamics with time-and state-dependent moving boundary". *International Journal of Robust and Nonlinear Control*, vol.25(2), pp.222-251, 2015.

[9] M. L. Delle Monache, & P. Goatin. "Scalar conservation laws with moving constraints arising in traffic flow modeling: an existence result". *Journal of Differential equations*, vol.257(11), pp.4015-4029, 2014.

[10] M. Diagne, N. Bekiaris-Liberis, & M. Krstic. "Time and State Dependent Input Delay Compensated Bang-Bang Control of a Screw Extruder for 3D Printing," *International Journal of Robust and Nonlinear Control*, vol.27(17), pp.3727-3757, 2017.

[11] M. Diagne, N. Bekiaris-Liberis, A. Otto, & M. Krstic. "Control of transport PDE/nonlinear ODE cascades with state-dependent propagation speed". *IEEE Transactions on Automatic Control*, vol.62(12), pp.6278-6293, 2017.

[12] L. Hu, R. Vazquez, F. Di Meglio, and M. Krstic, "Boundary exponential stabilization of 1-D inhomogeneous quasilinear hyperbolic systems". *SIAM Journal of Control and Optimization*, vol.57, pp. 963-998, 2019.

[13] I. Karafyllis, N. Bekiaris-Liberis, & M. Papageorgiou. "Feedback Control of Nonlinear Hyperbolic PDE Systems Inspired by Traffic Flow Models". *IEEE Transactions on Automatic Control*,vol.64(9), pp.3647-3662, 2018.

[14] S. Koga, & M. Krstic, "Arctic sea ice temperature profile estimation via backstepping observer design". *In 2017 IEEE Conference on Control Technology and Applications (CCTA)*, pp. 1722-1727, 2017.

[15] S. Koga, D. Straub, M. Diagne, & M. Krstic. "Thermodynamic Modeling and Control of Screw Extruder for 3D Printing". *In 2018 Annual American Control Conference (ACC)*, pp. 2551-2556, 2018.

[16] C. Lattanzio, A. Maurizi, & B. Piccoli. "Moving shockwaves in car traffic flow: a PDE-ODE coupled model". *SIAM Journal on Mathematical Analysis*, vol.43(1), pp.50-67, 2011.

[17] M. Treiber, & A. Kesting. "Traffic flow dynamics: data, models and simulation". *Physics Today*,vol.67(3), pp.54, 2014.

[18] D. Tsubakino, M. Krstic, & T. R. Oliveira, "Exact predictor feedbacks for multi-input LTI systems with distinct input delays". *Automatica*, vol.71, pp.143-150, 2016.

[19] S. Villa, P. Goatin, & C. Chalons. "Moving bottlenecks for the Aw-Rascle-Zhang traffic flow model". *Discrete and Continuous Dynamical Systems-Series B*, vol.22(10), pp.3921-3952, 2016.

[20] J. Wang, S. Koga, Y.Pi, & M. Krstic. "Axial Vibration Suppression in a Partial Differential Equation Model of Ascending Mining Cable Elevator". *Journal of Dynamic Systems, Measurement, and Control*, vol.140(11), 111003, 2018.

[21] H. Yu, and M. Krstic, "Traffic congestion control for Aw-Rascle-Zhang model," *Automatica,* vol.100, pp.38-51, 2019.

[22] H. Yu, S. Koga, & M. Krstic. "Stabilization of Traffic Flow With a Leading Autonomous Vehicle," *In ASME 2018 Dynamic Systems and Control Conference,* American Society of Mechanical Engineers, 2018.

[23] H. Yu, and M. Krstic. "Varying Speed Limit Control of Aw-Rascle-Zhang Traffic Model," *In 2018 21st IEEE International Conference on Intelligent Transportation Systems(ITSC),* pp. 1846-1851, 2018.

[24] L. Zhang, C. Prieur, & J. Qiao. "PI boundary control of linear hyperbolic balance laws with stabilization of ARZ traffic flow models". *Systems & Control Letters*, vol.123, pp.85-91, 2019.